

RSC Advances



This is an *Accepted Manuscript*, which has been through the Royal Society of Chemistry peer review process and has been accepted for publication.

Accepted Manuscripts are published online shortly after acceptance, before technical editing, formatting and proof reading. Using this free service, authors can make their results available to the community, in citable form, before we publish the edited article. This *Accepted Manuscript* will be replaced by the edited, formatted and paginated article as soon as this is available.

You can find more information about *Accepted Manuscripts* in the [Information for Authors](#).

Please note that technical editing may introduce minor changes to the text and/or graphics, which may alter content. The journal's standard [Terms & Conditions](#) and the [Ethical guidelines](#) still apply. In no event shall the Royal Society of Chemistry be held responsible for any errors or omissions in this *Accepted Manuscript* or any consequences arising from the use of any information it contains.

ARTICLE

Fabrication of concentric microarrays for self-assembly and manipulation of particle distribution

Cite this: DOI: 10.1039/x0xx00000x

Received 00th xxxx,
Accepted 00th xxxx

DOI: 10.1039/x0xx00000x

www.rsc.org/

L. K. Bera,^a Ong Kiansoo^a and Wong Zheng Zheng^a

We demonstrate using micro patterned surface composed of concentric circular array of SiO₂ and Si layer to distribute particles from edge to center and reduce the coffee stain effect from a colloidal or suspended solution droplet after natural evaporation by self assembly process over the array. The concentric circular alternative SiO₂/Si layer array with 3 μm width of each layer and depth of 400 nm surface is nonhomogeneous due to the presence of alternative hydrophilic (SiO₂)/hydrophobic (Si) and 400 nm surface roughness variation, respectively. The droplet diameter, contact angle and droplet height change more rapidly from the top of such surface compared to plain Si/SiO₂ during natural evaporation. The depinning process, capillary force and the Marangoni convection are the likely drying mechanisms to advect particles in the droplet for even distribution on top and side wall of the SiO₂ ring and thus minimize problems associated with the “coffee-stain” effect and provide better distribution when dispensed from a solution. The particle distribution is restricted to the top of the circular rims and sides or the floor of the space between the rings depending on the surface energy of the ring surfaces, structural geometry and natural evaporation of droplet.

Introduction

Many biological fluids are suspensions or colloids in a base liquid. Cells, vesicles and chemically functionalized nanoparticle solutions fall under this category. There are applications where a uniform distribution of the suspended particles on a surface is desired. Some examples of applications are micro patterned arrays of biochip for bioreactions with targeting probes such as antigens,¹ antibodies,² oligonucleotides,³ binding proteins,⁴ aptamers,⁵ receptors,⁶ and quantum dots⁷ immobilized on the surface. Generally these particles are conjugated with other materials such as proteins and Deoxyribonucleic acid (DNA). For assay applications, the particles need to be localized on the substrate. Several methods have been developed for arraying beads onto a flat surface. Some examples (or methods of obtaining) are of well ordered structures through the use of (i) porous film,⁸ (ii) electrostatic and capillary forces, (iii) dielectrophoresis, (iv) template-assisted self-assembly, (v) electrodeposition of adhesives, (vi) crosslinking, (vii) bead array assays for direct hybridization⁹ and (viii) hydrophobic interactions¹⁰ etc.

The hydrophobic interactions process is the most explored area of surface modification for spot probe assay experiments. There are several techniques such as, biologically inspired, fibres and textiles, phase separation, crystal growth, amphiphilic inorganic materials, nanostructured crystals, differential etching, diffusion-limited growth processes, lithographic techniques, aggregation/assembly of particles, and templating etc. are extensively studied by several research groups for hydrophobicity of the surfaces¹¹. Even though microarray assay technology is quite matured by adopting the suitable technologies as mentioned above but there are a number of effects that remain unresolved. For example, the signal intensity is higher at the edges and lower at the centre of a probe spot. Therefore, uniform distribution of the colloidal particles or vesicles is very important for minimizing saturation of the detector during fluorescence imaging. During drying the particles/vesicles tend to aggregate at the edge of the droplet which is commonly known as the “coffee stain” problem¹⁴ which causes doughnut patterns. The presence of coffee stain effect ring-shaped intensity pattern creates issues on correct analysis of probe spot. Very high intra-spot standard deviation occurs and existing image analysis tools do not equip with algorithms that are capable to minimize/eliminate such doughnut patterns effect. For microarrays on solid supports are generally glass slides. In many applications the surface of

^a Institute of Materials Research and Engineering (IMRE)
3, Research Link
Singapore 117602.
Email:beralk@imre.a-star.edu.sg

glass slides treated with different chemistries such as epoxy, amino-silane, poly-L-lysine, and streptavidin etc.¹⁵⁻¹⁷ Hydrogels coated glass slides are also used for immunoassays because the gel itself supports for binding the probes through moieties.¹⁸ However, for polymer/lipid vesicles or other bio applications there are requirements only to use physisorption and no chemical tailoring to bind these spheres covalently to the substrate so that no moieties are necessary on the surface of the vesicles that could be covalently bound to the surface. In this context, we study nonhomogeneous alternating hydrophilic (SiO_2)/hydrophobic (Si) surface (with 3 μm width of each and 400 nm trench depth from SiO_2 to Si) obtained using single-mask lithography followed by dry etching of SiO_2 for coffee stain reduction and uniform distribution of particle after natural evaporation.

Experimental

Two different materials SiO_2 and Si were employed to examine the natural evaporation of water droplets from homogeneous and nonhomogeneous surfaces, respectively. The surface of SiO_2 substrate is inherently hydrophilic and homogenous. The nonhomogeneous surface is an alternating SiO_2 and Si concentric circular structure. The design of concentric ring structure consists of SiO_2 ring and followed by Si trough. The width of each SiO_2 ring crest and Si trough is 3 μm i.e. the pitch is 6 μm . The single device comprises 165 numbers of SiO_2 ring crests and Si troughs. The diameter of single device is $\sim 1\text{mm}$. The depth of SiO_2 to Si is 400nm. The concentric SiO_2 /Si ring structure was fabricated using the single-mask photo lithography and dry etching process. The starting substrate was 100mm Si(100) wafer. After standard wafer cleaning thermal oxidation process performed to achieve 400nm of SiO_2 . The SiO_2 thickness on top of Si wafer has been verified using ellipsometer. The starting substrate was thermally grown 400nm SiO_2 on 100mm diameter <100> Si substrate. The top silicon dioxide layer of thickness 400nm etching process performed by RIE in an Oxford PlasmaLab80 system using 25sccm of Ar and 25sccm CHF_3 at room temperature with the pressure of 30 mTorr and RF power 100W, respectively. After dry etching the remaining photo resist and etch by-product was cleaned using piranha solution at 140 $^\circ\text{C}$. Substrate with concentric circular ring structure and plain Si/SiO_2 substrate was used to study the polystyrene particle distributions after droplet evaporation. The working colloidal fluid is a mixture of fluorescently loaded polystyrene beads with 200nm and 50nm diameter in deionised (DI) water. The excitation wavelength of the fluorescent loaded polystyrene particle is 441 nm. After excitation the particle radiate red emission of wavelength 486nm. The volume of the fluid used for droplet evaporation is 0.5 μL . Contact angles, contact diameters and centre heights of evaporating droplets were measured using an imaging system which consist of a CMOS camera (ARTCAM-300MI, Art-Ray Corporation, VA, USA), micropipettes (P2, Gilson, Inc., WI, USA), a magnifying lens (70 mm F2.8, EX DG, SIGMA Corporation, NY, USA), a halogen lamp (400W, 3M Overhead Projectors, MN, USA) and a computer with an installed frame grabber. The distribution of particles was characterized using scanning electron microscopy (SEM, XL-30, Philips Corp.) at an acceleration voltage of 20 kV.

Results and discussions

Fig. 1 shows the schematic of plain and micro patterned Si/SiO_2 substrates for particle distribution after natural evaporation, respectively.

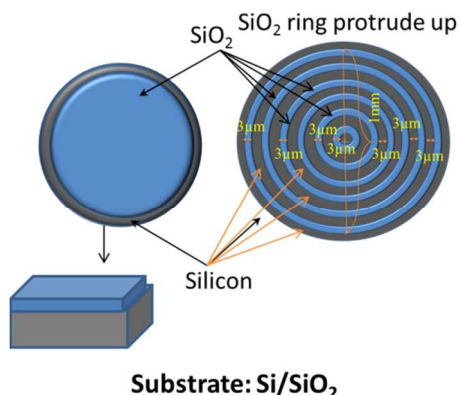


Fig. 1 Schematic of plain and micro patterned Si/SiO_2 substrate for particle distribution.

Micro pattern substrate is a concentric ring structure comprises hydrophilic SiO_2 protrusion followed by hydrophobic Si troughs. The concentric structure has multiple rings with outer diameter 1 mm in length. Droplets with 0.5 μL volume are dispensed on both substrates. The chosen volume of dispensed liquid (0.5 μL) has been based on several test runs for confinement of liquid within the outer ring. The images of droplets on both substrates are shown in Fig. 2 immediately after dispensation without allowing any time gap for evaporation.

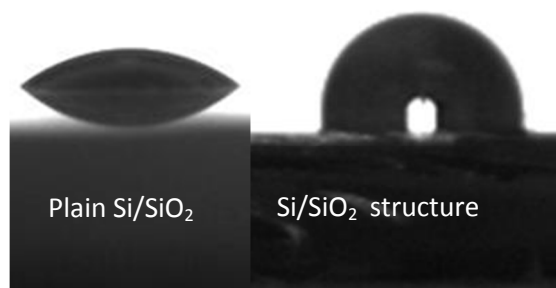

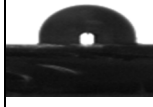


Fig. 2 Droplet shape on plain and micro ring pattern Si/SiO_2 substrate.

The contact angle, contact line diameter and height at the center of the droplets are shown in table 1. The contact angle measurement shows that the patterned substrate (102 degree) is apparently more hydrophobic than the plain Si/SiO_2 substrate (38 degree). The experiments have been repeated 3 times and the tabulated data are mean value with $\pm 5\%$ variation.

Table 1. Contact angle, contact diameter and droplet height at the center at evaporation time $t=0$ min.

Substrate	Droplet image at $t=0$ min	Con. angle (deg)	Con. diameter (mm)	Height at centre (mm)
Plain Si/SiO ₂		38.9	1.535	0.199
Micro patterned Si/SiO ₂ ring structure		102.6	0.95	0.373

The combined effect of surface topography and concentric alternating multiple hydrophilic/hydrophobic SiO₂/Si ring structure creates such hydrophobic surface. The contact diameter is shorter for patterned substrate and thus droplet height is higher compared to plain surface for an equal volume of droplet (droplet volume is 0.5 μ L). The shape of the droplet on patterned substrate is much more spherical than on smooth flat Si/SiO₂ surface due to the surface topography. A footage at the base of a droplet on patterned surface can be observed in Figure 2. In this study the dimension of the microstructure was selected to achieve Wenzel sticky states where droplets wet the “valley” patterned area for particle distribution. The base footage image as seen in Fig. 2 proofs that water droplet completely wets the textured surface which is known as “Wenzel state” after dispensing the liquid. In this state, since the air pockets are thermodynamically not stable, liquid begins to nucleate wetting layer from the base of the drop on substrate and form mushroom like shape as seen in Figure 2.

The natural evaporation of droplet from both surfaces have been investigated using real time monitoring of contact angle, contact diameter and droplet height. Fig. 3 shows a comparison of the normalized diameter plotted with normalized droplet evaporation time on both the surfaces.

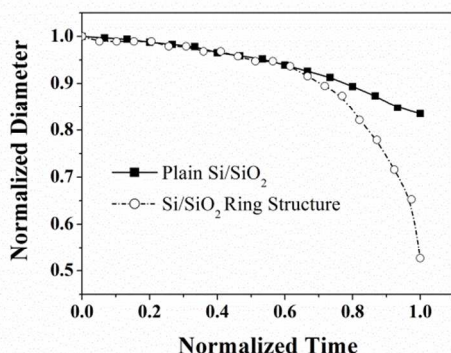


Fig. 3 Comparison of time dependent contact diameter of naturally evaporated colloidal fluid droplet from plain Si/SiO₂ surface and concentric Si/SiO₂ ring structure.

The diameter remains almost unchanged till about 50% of the total evaporation time which is the initial mode of an evaporating droplet on these two substrates. For the plain Si/SiO₂ substrate, a monotonous reduction of diameter is observed, and the initial wetting diameter of the droplets on this surface decreases $\sim 15\%$ until the droplet completely dries out. On the other hand, a rapid diameter reduction observed after 50% of evaporation time in the case of the Si/SiO₂ ring patterned substrate.

In order to investigate the contact line movement, the time-dependent edge shrinking velocity which is related to the rate of decrease of droplet diameter dD/dt for an evaporating droplet on both substrate surfaces has been plotted as shown in Fig. 4. (the plotted data are dD/dt derived from mean values of 3 experimental runs at each temporal point)

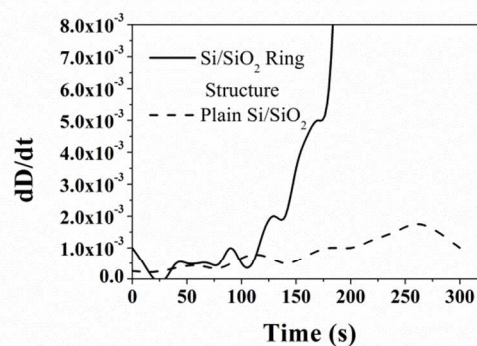


Fig. 4 Droplet edge shrinking velocities on plain Si/SiO₂ and concentric Si/SiO₂ ring structure surface.

In the case of the pattern surface several small peaks appear during the initial mode of evaporation when the diameter remains almost fixed. All these peaks are due to the inward movement of contact line during evaporation and thus rapid droplet diameter reduction occurs during evaporation. In contrast, the time-dependent edge shrinking velocity on plain Si/SiO₂ surface exhibits no such dominant peaks which is probably due to the slow process of droplet diameter reduction with evaporation time and the contact line was fixed during most of the evaporating time as illustrated in figure 3. It is noted that the edge shrinking velocity of the droplet on ring structure is nonlinear behaviour and its magnitude becomes extremely large at the end of evaporation whereas for the plain Si/SiO₂ surface, the behaviour is more linear. Time evolution of the droplet height was investigated to understand the effect of surface homogeneity (topography and hydrophobic/hydrophilic) during evaporation. The droplet height from both surfaces were investigated with evaporation time as shown in Fig. 5.

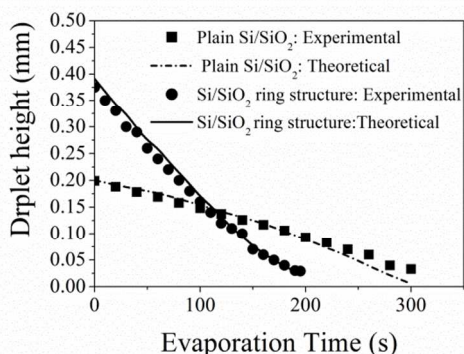


Fig. 5 Time evolution of droplet height plotted from plain Si/SiO₂ and concentric Si/SiO₂ ring structure.

The droplet height reduction is dependent on contact angle as a function of time and the contact-line radius,

$$h(r,t) = \sqrt{\frac{R^2}{\sin^2 \theta} - r^2} - \frac{R}{\tan(\theta)} \quad 1$$

where θ is the contact angle and R is the contact-line radius.¹⁴ At $r=0$, i.e. at the center of the droplet the height is

$$h(0,t) = R \tan\left[\frac{\theta(t)}{2}\right] \quad 2$$

For both the surfaces theoretical value (dashed and solid line) is quite close to the experimental data as depicted in figure 5 for plain Si/SiO₂ and pattern substrate, respectively. A trivial variation was observed probably due to the surface nonhomogeneity and accuracy limitation of experimental data collection. Initial droplet height on Si/SiO₂ ring structure is higher but it reduces much faster than plain Si/SiO₂ surface. Smaller droplet diameter and higher contact angle on patterned ring structure exhibit larger surface area to volume ratio. The larger contact angle and patterned geometry increase liquid–air interface. Therefore, both smaller droplet size and larger liquid–air interface promote faster evaporation on pattern substrate compared to plain Si/SiO₂ substrate.

Besides contact angle and larger surface area to volume ratio, the capillary forces from alternating hydrophobic Si and hydrophilic SiO₂ layers micro ring architecture also influence the drying effect and particle distribution on to the substrate surface during evaporation. Figure 6 (a), (b) and (c) demonstrated the particle distribution on plain and ring pattern Si/SiO₂ surface.

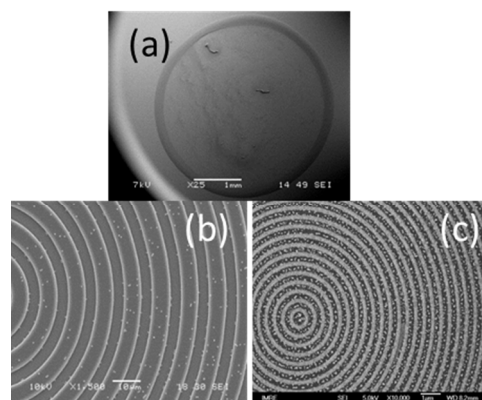


Fig. 6 SEM images of particle after natural evaporation (a) on plain SiO₂ substrate after evaporation of colloidal solution with 200nm polystyrene bead, (b) Si/SiO₂ ring structure after evaporation of colloidal solution with 200nm polystyrene bead, (c) Si/SiO₂ ring structure after evaporation of colloidal solution with 50nm polystyrene bead.

A significantly thick outer stain ring is observed, resulting from a pileup of polystyrene particles near droplet contact line similar to coffee stain effect on plain Si/SiO₂ substrate (Fig 6(a)). The particles pileup phenomenon is due to the development of internal fluid flow within the droplet along outward radial direction, effectively advecting particles towards the wetting line during evaporation. This flow pattern arises because of pinning and maximum evaporation flux at the wetting line as explained by Deegan et al.¹⁴ and Hu and Larson.¹⁹ In contrast, the ring structure shows an even distribution of the particles under the liquid droplet (Figure 6(b) and (c)). Although some particles still accumulate at the edge of the drop during the initial pinned stage, a significant number of them are distributed over the entire patterned structure. The droplet diameter on such patterned surface reduces continuously faster after 50% of total evaporation time than plain Si/SiO₂ surface as seen in Fig. 3. During this phase, the contact line continually switches between a pinned and a depinned state at alternating hydrophilic (SiO₂) and hydrophobic (Si) ring. In this experiment the drop volume is 0.5 μ L and such a microdrop, when located on a step at the boundary of hydrophilic SiO₂ region and a hydrophobic Si region, progressively moves towards the hydrophilic SiO₂ region due to the dominance capillary forces over gravity.²⁰ During evaporation, the liquid-solid wetting line creates local rise of the surface tension in the liquid which reduces surface flow, and as a result the liquid moves outward first and then turns back due to Marangoni effect. Generally the outward liquid flow is parallel to the substrate surface but the inward flow is nearly parallel to the vapor liquid interface which drags the particle in the inward direction.²¹ Thus the combined effect of depinning process, capillary force and the Marangoni convection drag acts to deposit particles on a regular concentric hydrophilic SiO₂ ring. During evaporation the suspended particles moves outwards or inwards due to the above-mentioned combined effects. Impeded by the ring side wall, particles are also deposited along the side of SiO₂ ring as shown in Fig. 6(b) and (c). The distribution of 200nm and 50nm beads on ring patterned Si/SiO₂ substrate after complete evaporation are similar which indicates that the distribution is determined by the substrate surface texture regardless of

beads size. However, the beads size must be smaller than the width of SiO₂ crest.

The real time droplet evaporation and saturation effect of detector have been studied using optical imaging system. The device was mounted onto an upright microscope (Olympus, BX51) with a mercury lamp attachment for fluorescence imaging. Charge-coupled device camera (Roper Scientific, Photometrics Cascade 512B and JVC, TK-C1481BEG) was used to capture the images and videos of the experiments for analysis. Fig 7(a) to (e) demonstrates the images of full device and zoom version at different time of evaporation. The contact diameter of evaporating droplet on concentric array of ring textured surface decreases with evaporation time. As an example, a substantial reduction of contact diameter occurs after 75 sec of evaporation as shown in Fig. 7(c). The distributions of fluorescently loaded polystyrene beads on ring structure are evenly arranged on top of the SiO₂ and some are situated at both inner and outer periphery of each SiO₂ ring (Fig. 7(d)) as explained earlier. Generally special sample/specimens preparation will be required for spectral imaging in order to avoid dramatic mismatches in intensity which causes saturation of the detector for the most concentrated probes such as from coffee stain ring while those of lower intensity can easily be lost in the noise floor. In this study the concentric Si/SiO₂ structure minimizes coffee stain effect, promotes self-assemble uniform distribution of particles after natural evaporation and naturally will reduce the saturation effect of detector.

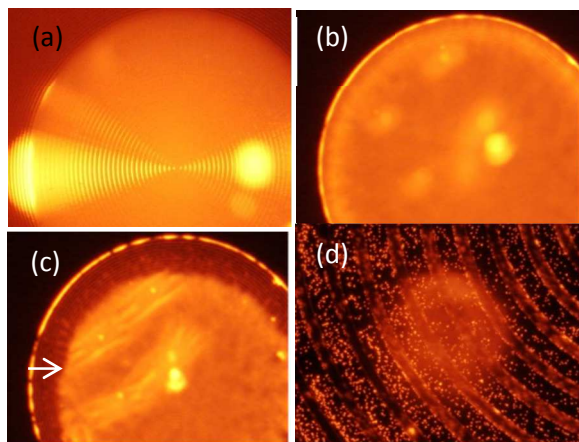


Fig. 7 Real time optical images of droplet evaporation and particle distributions on Si/SiO₂ ring structure (a) after droplet dispense (b) after 45sec of evaporation, (c) after 75 sec of evaporation and (d) Zoomed version after complete evaporation.

Conclusions

Micro patterned surface composed of concentric circular array of SiO₂ and Si layer have potential for uniform distribution of particles and reduction of the coffee stain effect from a colloidal or suspended solution droplet after natural evaporation by self assembly process. The concentric circular alternating SiO₂/Si layer array with 3μm width of each layer and depth of 400nm surface is nonhomogeneous due to the presence of alternating hydrophilic (SiO₂)/hydrophobic (Si) and 400nm surface roughness variation, respectively. Such

nonhomogeneous surface leads to a faster evaporation rate, faster reduction of contact angle and droplet diameter. The combined effect of depinning process, capillary force and the Marangoni convection leads to an even distribution of particles on the top and side wall of the SiO₂ ring and thus minimize problems associated with the “coffee-stain” effect and provide better distribution of particles dispensed from a solution. Consequently, the structure allows uniform distribution of signal and avoids saturation of detectors when a fluorescent sample is inspected by conventional fluorescent analyzers.

Acknowledgements

The authors wish to deeply thank Dr Madanagopal V Kunnavakkam, ST Microelectronics Singapore for very helpful comments and discussions.

References

- 1 P. Montagne, P. Varcin, M.L. Cuilliere, J. Duheille, *Bioconjug. Chem.*, 1992, **2**, 187.
- 2 R. Bellisario, R.J. Colinas, K.A. Pass, *Early Hum. Dev.*, 2001, **64**, 21.
- 3 Y. Kohara, H. Noda, K. Okano, H. Kambaba, *Nucleic Acids Res.* 2002, **30**, e87.
- 4 A.S. Brodsky, P.A. Silver, *Mol. Cell. Proteomics*, 2002, **1**, 922.
- 5 H.Y. Zhu, J.D. Suter, I.M. White, F.D. Fan, *Sensors*, 2006, **6**, 785.
- 6 M.A. Iannone, T.G. Consler, K.H. Pearce, J.B. Stimmel, D.J. Parks, J.G. Gray, *Cytometry*, 2001, **44**, 326.
- 7 Q. Ma, T.-Y. Song, P. Yuan, C.Wang, X.-G. Su, *Colloids Surf.*, 2008, **B 64**, 248.
- 8 J. Lee, O. Kim, J. Jung, K. Na, P. Heo, and J. Hyun, *Colloids and Surfaces B: Biointerfaces*, 2009, **72**, 173.
- 9 <http://www.illumina.com/support/documentation.ilmnix>
- 10 F. Fan, and K. J. Stebe, *Langmuir* 2004, **20**, 3062.
- 11 Paul Roach, Neil J. Shirtcliffe and Michael I. Newton, *Soft Matter*, 2008, **4**, 224–240
- 12 A. L. Dubov1, J. Teisseire and E. Barthel, *EPL*, 2012, **97**, 26003
- 13 J. Drelich, J. L. Wilbur, J. D. Miller and G. M. Whitesides, *Langmuir* 1996, **12**, 1913-1922
- 14 R. D. Deegan, O. Bakajin, T. F. Dupont, G. Huber, S. R. Nagel and T. A. Witten, *Nature*, 1997, **389**, 827.
- 15 W. Kusnezow, A. Jacob, A. Walijew, F. Diehl and J. D. oheisel, *Proteomics*, 2003, **3**, 254–264.
- 16 E. W. Olle, J. Messamore, M. P. Deogracias, S. D. McClintock, T. D. Anderson and K. J. Johnson, *Exp. Mol. Pathol.*, 2005, **79**, 206–209.

17 C. Wingren, J. Ingvarsson, L. Dexlin, D. Szul and C. A. K. Borrebaeck, *Proteomics*, 2007, 7, 3055–3065.

18 Huiyan Li, Rym Ferial Leulmi and David Juncker, *Lab Chip*, 2011, 11, 528–534

19 H. Hu and R. G. Larson, *J. Phys. Chem. B* 2002, 106, 1334.

20 M. K. Chaudhury and G.M. Whitesides, *Science*, 1992, 256, 1539

21 Xuefen Xu and Jian Bin, *Proceeding of CIST* 2008. 186